UPPER-REGIME PLANE BED

By P. Y. Julien,[1] Member, ASCE, and Y. Raslan[2]

ABSTRACT: The analysis of a laboratory and field data set for sand-bed channels defines the characteristics of upper-regime plane bed with sediment transport. The occurrence of upper-regime plane bed relates to the laminar sublayer thickness δ and depends on shear velocity u_*, median grain size d_{50}, and grain shear Reynolds number R_*. Two different boundary conditions are recognized: (1) Transition to hydraulically smooth when $R_* < 11.6$; and (2) transition to hydraulically rough when $R_* > 11.6$. In the first case, upper-regime plane bed is obtained when $u_*^2 \cong g\delta$, where g is the gravitational acceleration. In the second case, upper-regime plane bed is observed when $d_{50} \cong 2\delta$. Temperature effects are possible when R_* approaches 11.6, which explains the observations on the Missouri River. Resistance to flow for plane bed with sediment transport increases with the Shields parameter.

INTRODUCTION

The complexity of bed-form configurations in sand-bed rivers continues to challenge engineers and scientists. The large number of dimensionless parameters describing the complex interactions between sediment particles and hydrodynamic forces contributes to the elusive understanding of bed forms and flow resistance in alluvial channels. Estimating river stage is quite important for irrigation, water supply, and flood protection; yet, accurate stage prediction depends on insufficient understanding of resistance to flow in alluvial channels.

Resistance to flow in alluvial channels has been associated with the surface roughness height k_s. For plane bed without sediment transport, the roughness height k_s corresponds to the coarser fractions of the bed sediment size distribution. For instance, Einstein and Barbarossa (1952) proposed the equivalent roughness $k_s = d_{65}$; Simons and Richardson (1966) proposed $k_s = d_{85}$; Kamphuis (1974) suggested $k_s = 2.5d_{90}$; and Bray (1982) proposed $k_s = 3.5d_{84}$ and $k_s = 6.8d_{50}$.

Complexities in alluvial sand-bed channels stem from the variety of bed-form configurations that arise under different flow conditions. Starting from plane bed without sediment transport, ripples, dunes, washed-out dunes, plane bed with sediment transport, antidunes, and chutes and pools develop in large experimental flumes as the flow intensity increases in magnitude over a bed of loose sand particles. Based on a large data set collected from laboratory flumes, Simons and Richardson (1966) forged a bed-form classification that recognizes lower and upper flow regimes. The transition between both regimes is called the upper-regime plane bed characterized by a plane bed surface with sediment transport.

Athaullah (1968) classified the flow regimes according to the Froude number and the relative bed roughness on a diagram that separates upper regime, transition, and lower regime. van Rijn (1984) classified the transition and the lower regime following a dimensionless particle diameter and a transport-stage parameter that expresses the ratio between excess grain shear stress and the critical shear stress for beginning of motion. Studies have considered the flow in the upper-regime plane bed since Vanoni and Brooks (1957) and Simons and Richardson (1961, 1966). The effects of sand gradation have been examined by Daranandana (1962), Nordin (1976), and Klaassen (1991). Other studies include Bogardi (1965), Nordin (1965), Engelund and Hansen (1967), Znamenskaya (1969), Williams (1970), Engelund and Fredsøe (1974), Shen et al. (1978), Brownlie (1982), van Rijn (1982), Wijbenga and Klaassen (1983), Paola et al. (1989), Wijbenga (1990), Best and Bridge (1992), Julien (1992), Wang and Larsen (1994), Bennett (1995), Julien and Klaassen (1995), and Nnadi and Wilson (1995).

Resistance to flow in alluvial channels involves two components: (1) Grain resistance due to surface roughness; and (2) form resistance induced by bed forms. Meyer-Peter and Müller (1948) and Einstein and Barbarossa (1952) advocated separation of the total bed-shear stress τ_0 into two components for grain shear stress τ_0' and for bed-form shear stress τ_0''. The notation with prime (′) and double prime (″) hereby refers to grain and form components, respectively. The complexity in the analysis of both components leads to a wealth of literature summarized in Engelund and Hansen (1967), van Rijn (1984), and Simons and Senturk (1992).

Julien and Klaassen (1995, 1997) observed that during floods, large sand-bed rivers do not necessarily reach upper-regime plane bed with $T = (\tau_0' - \tau_c)/\tau_c = 25$. Accordingly, renewed interest emerged to define the physical conditions required for upper-regime plane bed. A particularly interesting feature of upper-regime plane bed arises from the simplifications induced by $\tau_0'' = 0$. Total resistance to flow for upper-regime plane bed is caused by grain resistance only, or $\tau_0 = \tau_0'$, and the effects of sediment transport on resistance to flow should then become apparent.

Objectives

This study of upper-regime plane bed with sediment transport particularly focuses on (1) determining the conditions of occurrence for the upper-regime plane bed; and (2) resistance to flow in upper-regime plane bed. In the foregoing analysis, attempts are made to delineate the flow conditions that separate lower and upper regimes. The transition zone between washed-out dunes and antidunes will be described by the scatter around the plane bed conditions.

An experimental study first investigates upper-regime plane bed using different particle sizes and a sediment mixture. The analysis is then extended to a field and laboratory data set to delineate the conditions for upper-regime plane bed and resistance to flow.

LABORATORY EXPERIMENTS

Experiments on resistance to flow for sand mixtures were carried out under controlled conditions of discharge, sediment size, slope, temperature, and flow depth. Numerous experiments on upper-regime plane bed were carried out in a 1.3-m-wide, 18-m-long, 0.6-m-deep flume that recirculates both water and sediment. Upper-regime plane bed deposits were clearly visible through the plexiglass sidewalls at the 7.2-m-

[1]Dept. of Civ. Engrg., Engrg. Res. Ctr., Colorado State Univ., Fort Collins, CO 80523.

[2]Nat. Water Res. Ctr., Nile Res. Inst., Elqanatir, 13621, Egypt; formerly, Grad. Student, Colorado State Univ., Fort Collins, CO.

Note. Discussion open until April 1, 1999. To extend the closing date one month, a written request must be filed with the ASCE Manager of Journals. The manuscript for this paper was submitted for review and possible publication on November 21, 1996. This paper is part of the *Journal of Hydraulic Engineering*, Vol. 124, No. 11, November, 1998. ©ASCE, ISSN 0733-9429/98/0011-1086–1096/$8.00 + $.50 per page. Paper No. 14443.

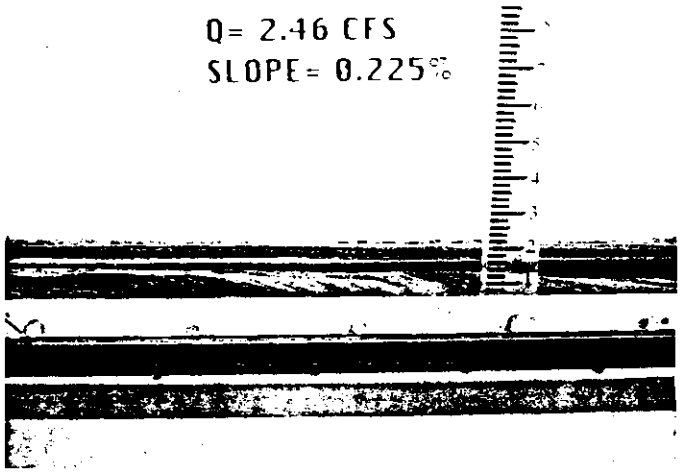

FIG. 1(a). Upper-Regime Plane Bed in 4-ft-Wide Laboratory Flume

long downstream part of the flume as shown in Fig. 1(a). A pump sustained adequate mixing of water and sediment at the upstream end of the recirculating flume. The flow was maintained constant at a rate up to 0.13 m^3/s and the flume bed slope could be adjusted up to 2%.

Two different sediment sizes were used: (1) A uniform fine white sand with particle size distribution shown in Table 1, d_{50} = 0.2 mm and specific gravity of 2.5; and (2) a uniform coarse black sand with particle size distribution shown in Table 1, d_{50} = 0.6 mm and specific gravity is 2.7. Table 1 also outlines the characteristics of the fine white sand and the coarse black sand. Equal volumes of fine and coarse sand were added together and mixed to provide additional runs with a black and white sand mixture. The size distribution of the sand mixture is also given in Table 1.

TABLE 1. Characteristics of Particle Size Distribution

Sand (1)	Color (2)	Specific gravity (3)	Angle of response in air (degree) (4)	Shape (5)	d_{35} (6)	d_{50} (7)	d_{90} (8)
Fine	White	2.5	35.5	Rounded	0.18	0.20	0.25
Coarse	Black	2.7	39.5	Angular	0.56	0.60	0.80
Mixture	Black/white	2.6	—	Mixed	0.23	0.40	0.55

The experiments with upper-regime plane bed were carried out for three particle sizes: (1) fine white sand, d_{50} = 0.2 mm; (2) coarse black sand, d_{50} = 0.6 mm; and (3) equal volume sand mixture, d_{50} = 0.4 mm. The upper-regime plane bed was obtained using the procedures detailed in Simons and Richardson (1966). The upper-regime plane bed with sediment transport was obtained when both the bed surface and water surface profiles remained flat and stable over a period of 3 h. The flow depth was measured using point gauges along the flume centerline and using staff gauges along the flume sidewalls. Sidewall and centerline measurements were almost identical.

A total of 28 runs were completed with 11 runs for fine sand, seven runs for coarse sand, and 10 runs for the sediment mixture. A summary of the measured data, with subscript p to designate upper-regime plane bed, for each run is presented in Table 2 with median grain size d_{50} (mm), flow discharge Q (m^3/s), flow depth h_p (m), energy slope S_p (m/m), mean flow velocity U_p (m/s), Froude number $F_p = U_p/\sqrt{gh_p}$, the Darcy-Weisbach bed friction factor for a moving bed f_p, the bed hy-

TABLE 2. Laboratory Data Summary for Upper-Regime Plane Bed

Run number[a] (1)	d_{50} (mm) (2)	Q (m^3/s) (3)	h_p (m) (4)	S_p (5)	U_p (m/s) (6)	F_p (7)	f_p (8)	R_b (m) (9)	u_{*p} (m/s) (10)	τ_{0p} (N/m^2) (11)	τ_{0p}/τ_c (12)	h_p/d_{50} (13)	d_* (14)	R_* (15)
(*a*) Fine sand														
1	0.20	0.130	0.136	2.332E-03	0.788	0.683	0.036	0.123	0.053	2.81	29.4	678	4.4	9.0
2	0.20	0.067	0.085	2.676E-03	0.640	0.699	0.041	0.080	0.046	2.10	21.9	426	4.4	7.8
3	0.20	0.074	0.082	2.252E-03	0.734	0.817	0.025	0.075	0.041	1.66	16.8	411	4.4	6.9
4	0.20	0.076	0.086	2.923E-03	0.728	0.792	0.035	0.080	0.048	2.29	24.0	430	4.4	8.1
5	0.20	0.076	0.081	4.083E-03	0.776	0.872	0.041	0.076	0.055	3.05	31.9	403	4.4	9.4
6	0.20	0.076	0.080	3.841E-03	0.784	0.885	0.037	0.075	0.053	2.83	29.6	400	4.4	9.0
7	0.20	0.057	0.077	2.752E-03	0.607	0.700	0.043	0.072	0.044	1.95	20.2	382	4.4	7.5
8	0.20	0.057	0.073	1.870E-03	0.635	0.750	0.024	0.067	0.035	1.23	12.3	365	4.4	5.9
9	0.20	0.057	0.062	4.098E-03	0.717	0.900	0.038	0.062	0.050	2.47	25.8	323	4.4	8.4
10	0.20	0.062	0.072	2.634E-03	0.706	0.838	0.028	0.067	0.042	1.73	17.8	361	4.4	7.1
11	0.20	0.062	0.070	4.182E-03	0.729	0.879	0.041	0.067	0.052	2.72	28.5	350	4.4	8.9
(*b*) Coarse sand														
1	0.60	0.026	0.056	3.160E-03	0.406	0.566	0.077	0.051	0.040	1.58	4.6	87	13.7	20.3
2	0.60	0.026	0.046	4.480E-03	0.460	0.681	0.075	0.045	0.045	1.99	5.7	77	13.7	22.8
3	0.60	0.026	0.043	4.782E-03	0.492	0.754	0.066	0.042	0.045	1.98	5.7	72	13.7	22.7
4	0.60	0.026	0.038	4.997E-03	0.561	0.917	0.046	0.037	0.043	1.81	5.2	63	13.7	21.7
5	0.60	0.029	0.052	2.574E-03	0.453	0.635	0.069	0.050	0.042	1.76	2.1	86	13.7	21.4
6	0.60	0.023	0.055	2.958E-03	0.347	0.473	0.103	0.054	0.039	1.55	4.5	91	13.7	20.1
7	0.60	0.023	0.037	5.118E-03	0.510	0.843	0.056	0.036	0.043	1.82	5.2	62	13.7	21.8
(*c*) Sediment mixture														
1	0.40	0.045	0.066	3.776E-03	0.567	0.700	0.058	0.063	0.048	2.33	11.1	163	9.0	16.4
2	0.40	0.040	0.058	3.023E-03	0.570	0.750	0.040	0.055	0.040	1.63	8.0	144	9.0	13.8
3	0.40	0.093	0.082	5.301E-03	0.934	1.045	0.037	0.077	0.063	3.98	18.4	203	9.0	21.5
4	0.40	0.093	0.091	3.405E-03	0.845	0.890	0.031	0.084	0.053	2.80	13.2	226	9.0	18.0
5	0.40	0.061	0.062	4.120E-03	0.817	1.050	0.028	0.058	0.048	2.14	11.2	154	9.0	16.5
6	0.40	0.076	0.075	3.799E-03	0.831	0.970	0.030	0.070	0.051	2.59	12.3	186	9.0	17.3
7	0.40	0.074	0.075	4.970E-03	0.804	0.934	0.043	0.072	0.059	3.48	16.2	188	9.0	20.1
8	0.40	0.070	0.075	4.405E-03	0.765	0.890	0.042	0.071	0.055	3.05	14.4	186	9.0	18.8
9	0.40	0.063	0.066	4.538E-03	0.783	0.970	0.036	0.062	0.053	2.76	13.1	163	9.0	17.9
10	0.40	0.069	0.069	4.344E-03	0.814	0.987	0.034	0.065	0.053	2.78	13.1	173	9.0	17.9

[a]In a 4-ft-wide flume.

draulic radius R_b (m), the shear velocity u_{*p} (m/s), the bed-shear stress τ_{0p} (Pa), the ratio τ_{0p}/τ_c of applied to critical shear stresses, the relative submergence h_p/d_{50}, the dimensionless particle diameter $d_* = d_{50}[(G - 1)g/\nu^2]^{1/3}$ given the specific gravity of sediment particles G, gravitational acceleration g, fluid kinematic viscosity ν, and the grain shear Reynolds number $R_* = u_* d_{50}/\nu$. Note that the kinematic fluid viscosity was calculated at $\nu = 1.17 \times 10^{-6}$ m^2/s from water temperature measurements near $T° = 14°C$. The Vanoni-Brooks method was used to correct for sidewall effects. The procedure is detailed in Julien (1995, p. 105) and calculations are available in Raslan (1994).

Observations and Results

The laboratory experiments on upper-regime plane bed summarized in Table 2 provided the following observations. First, the runs with coarse sand required a longer time to reach equilibrium. This is because the values of τ_{0p}/τ_c for coarse sand ($\tau_{0p}/\tau_c \cong 5$) were much lower than those for fine sand ($\tau_{0p}/\tau_c \cong 20$). Sediment transport rates for fine sand far exceed the transport rates for coarse sand, and equilibrium conditions could be reached faster for fine sand. Second, the flume slope required for upper-regime plane bed was steeper for coarse sand than for fine sand. The flow depth for coarse sand was significantly less than the flow depth for fine sand. The flow velocity was also less for coarse sand. Third, in the case of graded sediment mixtures, a view of particle motion near the bed surface in Fig. 1(b) shows that the stationary bed particles are covered by a thin film of fine sand particles located in the interstices between coarse sand grains. The presence of fine particles at the bed interface enhances the motion of coarse sands in the moving bed layer. This surface smoothing phenomenon for graded sediment mixtures is also conducive to lamination and stratification of sedimentary deposits clearly visible in Fig. 1(a) and as explained in Julien et al. (1993).

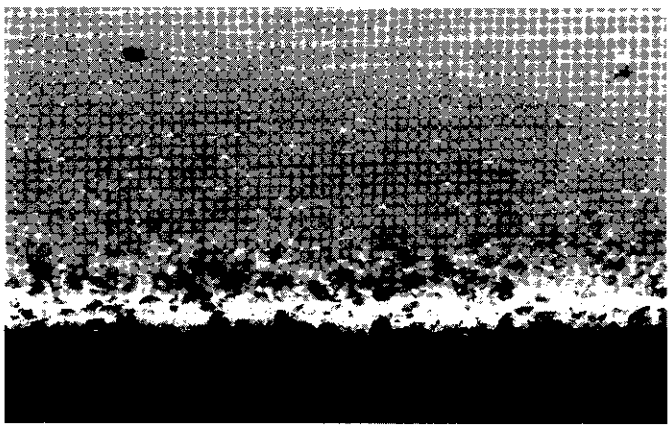

FIG. 1(b). Particle Interaction in Bed Layer for Upper-Regime Plane Bed

A quantitative analysis of the data collected in the 1.33-m-wide flume shows the effects of grain size and nonuniformity of bed material on resistance to flow and related hydraulic and sediment parameters for the occurrence of upper-regime plane bed. From the experimental data in Table 2, plane bed with sediment transport occurs under the same range of Froude numbers from 0.6 to 1.0. No trend could be detected when plotting the Froude number F_p against the relative submergence defined as the ratio of flow depth h_p to median grain size d_{50}.

A Shields diagram of the laboratory data in Fig. 2 indicates that all size particles are in motion and values of R_* reflect the transition zone between turbulent flow over smooth boundary ($4 < R_* < 11.6$) and turbulent flow over rough boundary ($11.6 < R_* < 70$). The value of the Shields parameter required to form plane bed with sediment motion is higher for fine sand than for coarse sand. Notice that the value of the grain Reynolds number approaches $R_* \cong 20$ when $d_s = 0.4$ and 0.6 mm.

The transport-stage parameter T has been defined by van Rijn (1984) as the ratio of excess grain shear stress to the critical shear stress, or $T = (\tau_0' - \tau_c)/\tau_c$. The relation between the relative roughness and the transport parameter T_p for upper-regime plane bed with $\tau_0' = \tau_{0p}$ is depicted in Fig. 3. The figure indicates that T_p gradually increases with h_p/d_{50}.

The relation between the Darcy-Weisbach bed friction factor f_p (which is equal to f' for upper-regime plane bed) and the sediment transport parameter T_p is shown in Fig. 4. Resistance to flow for a graded sand mixture lies in a position closer to flow resistance for the fine fraction rather than the coarse fraction. The mixture thus has a slightly higher friction factor than that of fine sand. This can be explained by the smoothing of the surface layer for the transport of sand mixtures as shown in Fig. 1(b). Since the rate of sediment transport increases with T_p, it would be misleading to conclude from Fig. 4 that resistance to flow decreases as sediment transport T_p increases simply because T_p is itself a function of h_p/d_{50} as shown in Fig. 3. This point will be discussed further in the foregoing analysis of an extended data set.

EXTENDED DATA ANALYSIS

Numerous field investigations in alluvial sand-bed rivers could be cited in addition to Beckman and Furness (1962),

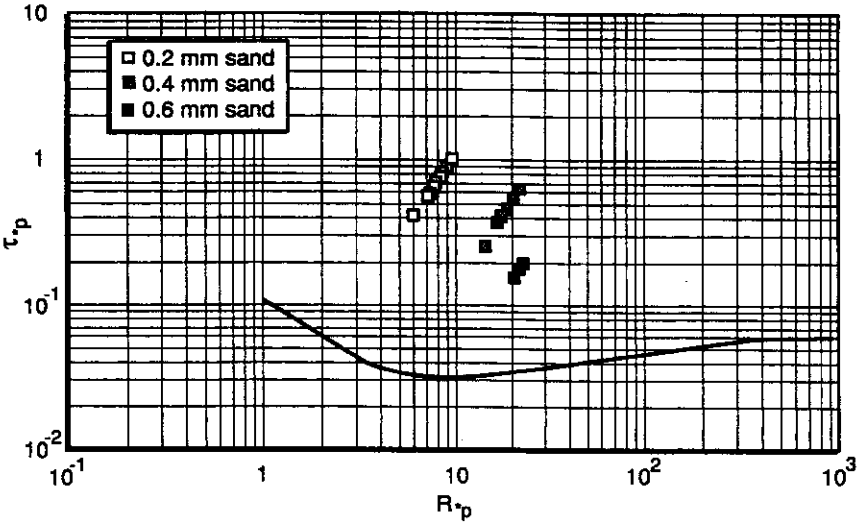

FIG. 2. Shields Diagram for Upper-Regime Plane Bed

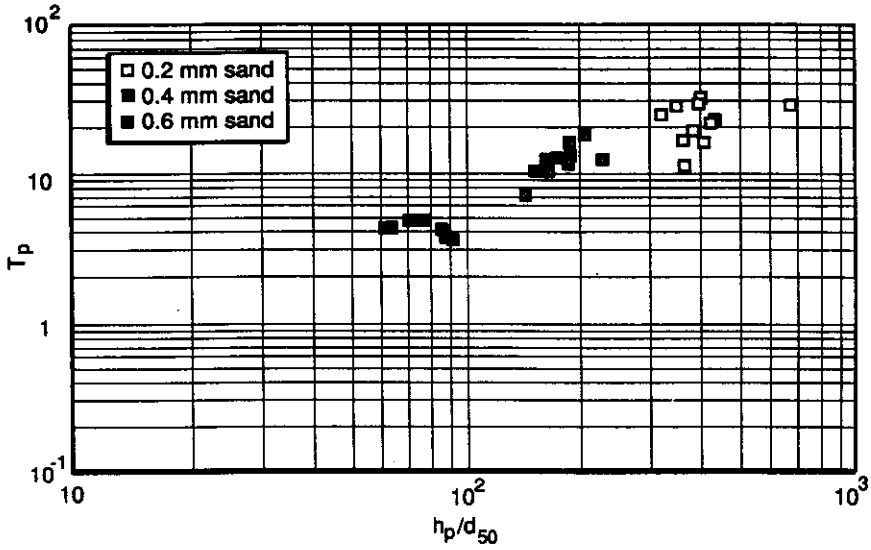

FIG. 3. Transport-Stage Parameter T_p versus Relative Submergence h_p/d_{50} for Upper-Regime Plane Bed

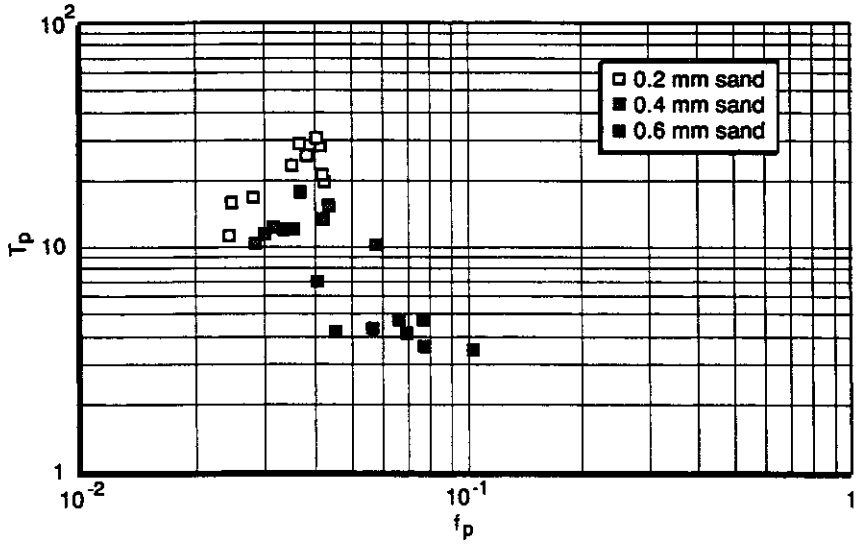

FIG. 4. Transport-Stage Parameter T_p versus Bed Friction Factor f_p for Upper-Regime Plane Bed

Nordin (1964), and Shen et al. (1978). Given that laboratory and field data sets have been compiled for a long period of time, a more comprehensive analysis of an extended data set is now considered. The data set has been extended to include the laboratory data of Chyn (1935), the U.S. Waterways Experiment Station [U.S. Army Corps of Engineers (USACE) 1936a,b], Jorissen (1938), Vanoni and Brooks (1957), Singh (1960), Guy et al. (1966), Simons and Richardson (1966), and Franco (1968). The field data set includes ACOP canals in Pakistan, the Missouri River, the Rio Grande, American canals, the Elkhorn, and the Niobrara rivers. A summary of relevant hydraulic and sediment transport parameters is presented in Table 3. The entire data set includes 174 upper-regime plane bed measurements (68 field and 106 laboratory) listed in Raslan (1994).

Analysis of Upper-Regime Plane Bed

The extended data set on upper-regime plane bed in Table 3 displays the following general characteristics. The Froude number for upper-regime plane bed is lower for field than for laboratory conditions. Field observations of the Froude number for plane bed range between 0.13 and 0.68. Comparatively higher values of the Froude number are required in the laboratory, typically 0.21–1.6. Values of the Darcy-Weisbach friction factor are quite comparable for both field and laboratory conditions. The sediment transport rate as indicated by τ_{0p}/τ_c is much larger for field data than for laboratory experiments. The wide range of values for these hydraulic and sediment parameters portrays upper-regime plane bed as a complex phenomenon that is particularly difficult to analyze because at $3 < R_* < 46$, turbulent flows in sand-bed channels are in the transition between hydraulically rough and hydraulically smooth boundaries.

The analysis of the extended data set first attempts to verify that the Froude number F varies with the relative submergence h/d_{50} as suggestd by Athaullah (1968). Relative submergence should separate field from laboratory conditions because at a given grain size, flow depths are much larger in rivers than in laboratory flumes. It is found in Fig. 5 that the Froude number does not necessarily decrease with relative submergence. Most rivers indeed have higher values of h/d_{50} and lower F, but low values of F have also been reported in the laboratory [e.g., Franco (1968)].

On a Shields diagram in Fig. 6, the data does not display any definite trend between laboratory and field data. In fact, very low values of the Shields number are possible under several laboratory conditions, while high values of the Shields are found in most rivers. Most values of the Shields number for

TABLE 3. Summary of Extended Field and Laboratory Data Set for Upper-Regime Plane Bed

Data set (1)	Number (2)	Q (m^3/s) (3)	h_p (m) (4)	S_p (cm/km) (5)	d_{50} (mm) (6)	F_p (7)	f_p (8)	R_* (9)	τ_{0p}/τ_c (10)	h_p/d_{50} (11)
Field										
ACOP	6	50–158	1.4–2.3	7–13	0.08–0.2	0.13–0.19	0.024–0.033	3.8–7.4	18–38	10,000–2,700
Niobrara	17	8–15	0.4–0.58	132–180	0.21–0.32	0.47–0.51	0.035–0.053	9.7–24	38–85	1,350–2,640
Missouri	1	937	2.8	16	0.22	0.32	0.012	9.7	37	12,380
American canals	2	3–12	1.3–1.8	6–11	0.1–0.35	0.14–0.17	0.018–0.02	3–15	8–17	3,800–19,100
Rio Grande	20	3–235	0.4–1.2	45–84	0.16–0.29	0.25–0.68	0.014–0.06	5–22	16–77	2,100–6,800
Elkhorn	22	158–385	1.3–2.0	31–47	0.23	0.33–0.48	0.011–0.03	12–20	40–59	5,500–8,800
Laboratory										
Franco	8	0.036	0.12–0.15	23–60	2.2	0.21–0.28	0.027–0.048	24–67	1.1–2.5	56–68
Simons	21	0.1–0.6	0.09–0.24	112–790	0.19–0.54	0.68–1.6	0.016–0.04	9–46	13–41	190–1,270
Julien-Raslan	28	0.02–0.13	0.04–0.14	187–511	0.2–0.6	0.47–1.0	0.024–0.10	6–22	4–31	62–678
Brooks	8	0.01	0.06–0.08	185–250	0.09–0.15	0.7–0.8	0.018–0.024	3–5	11–17	410–970
Vanoni-Brooks	3	0.03–0.1	0.06–0.17	107–276	0.14	0.6–0.8	0.017–0.03	5.2–5.5	16–19	450–520
Jorissen	5	0.005–0.02	0.05–0.08	111–332	0.91	0.42–0.58	0.034–0.08	23–34	1.3–2.7	38–86
Singh	12	0.003–0.013	0.015–0.046	150–1,400	0.62	0.55–1.2	0.034–0.057	11–42	1.4–15	25–75
Chyn	2	0.012–0.016	0.05–0.06	120–152	0.79	0.51	0.03–0.04	21–22	1.5–1.66	65–80
WES[a]	19	0.009	0.074	100	0.65–0.85	0.42–0.48	0.026–0.029	15–19	1.17–1.66	87–118
Total	174	0.005–385	0.04–2.8	6–1,400	0.08–0.91	0.13–1.6	0.011–0.10	3–67	1.17–85	30–27,000

[a]U.S. Waterways Experiment Station.

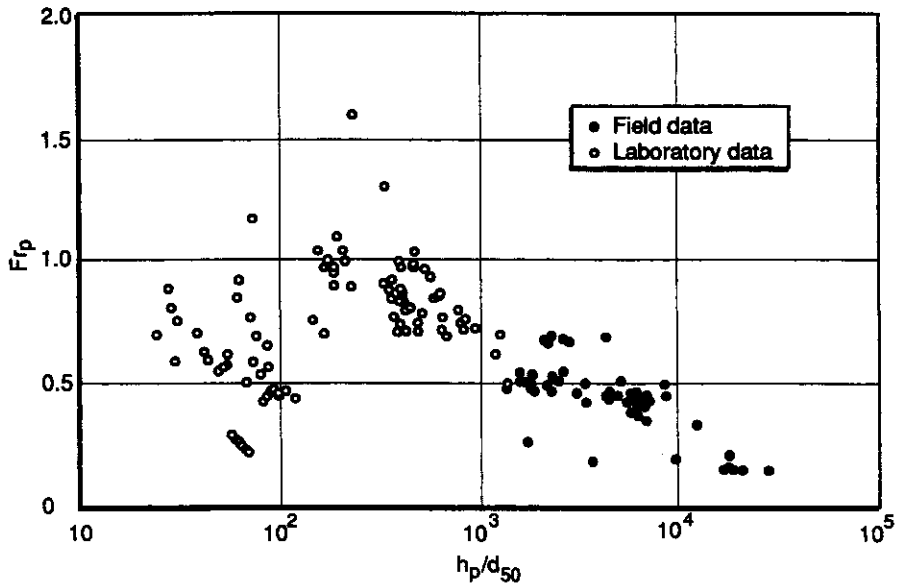

FIG. 5. Froude number F_p versus Relative Submergence h_p/d_{50} for Upper-Regime Plane Bed

field data range from $0.5 < \tau_{*p} < 2$. This is particularly true for both laboratory and field data when $R_* < 11.6$.

van Rijn (1984) suggested that upper-regime plane bed occurs when the transport-stage parameter T_p defined as $T_p = (\tau_0' - \tau_c)/\tau_c = 25$. The relationship between T_p and the relative submergence h_p/d_{50} is shown in Fig. 7. The data points indicate a trend where T_p increases with an increase in relative submergence. Field measurements correspond to upper values of both T_p and h_p/d_{50}. Typically, the upper-regime plane bed occurs when $20 < T_p < 100$ for field observations and when $0.1 < T_p < 30$ in the laboratory. Upper-regime plane bed does not occur at a single value of the transport-stage parameter T_p. This corroborates the statement that large sand-bed rivers do not necessarily reach upper-regime plane bed when $T_p = 25$ (Julien and Klaassen 1995).

The relationship between the transport-stage parameter T_p and the grain Reynolds number R_* in Fig. 8 shows the effect of the laminar sublayer thickness. The results corroborate those of the Shields diagram in Fig. 6. Distinct symbols are used to separate the data points into transition to hydraulically smooth boundary for values of $R_* < 11.6$ and transition to hydraulically rough boundary for $R_* > 11.6$. The value of T_p varies from $10 < T_p < 70$ when $R_* < 11.6$, but there is no trend whatsoever with R_* for transition to hydraulically rough, $R_* > 11.6$. Notice that the term transition hereby refers to hydraulic roughness conditions described by R_* and should not be confused with transition from lower to upper regime.

It is becoming clear that two types of boundary conditions must be recognized and must be analyzed separately: (1) Transition to hydraulically smooth boundary when $4 < R_* < 11.6$; and (2) transition to hydraulically rough boundary when $11.6 < R_* < 70$. The relationship between the Shields parameter τ_* and the grain Reynolds number R_* is such that $\tau_* d_*^3 = R_*^2$, where the dimensionless particle diameter $d_* = d_{50}[(G - 1)g/\nu^2]^{1/3}$ given the median grian size d_{50}, the specific gravity of a sediment particle G, the gravitational acceleration g, and the fluid kinematic viscosity ν.

Transition to Hydraulically Smooth Boundary $4 < R_* < 11.6$

In the case of transition to hydraulically smooth boundary $4 < R_* < 11.6$, the transport-stage parameter T_p varies between 10 and 70, as shown in Fig. 8. Equivalent results are obtained in Fig. 6 with $0.5 < \tau_{*p} < 2.0$.

When $R_* < 11.6$, one would expect that the grain diameter does not influence the boundary conditions. Through dimensional analysis, the combination of parameters τ_*, R_*, and d_*

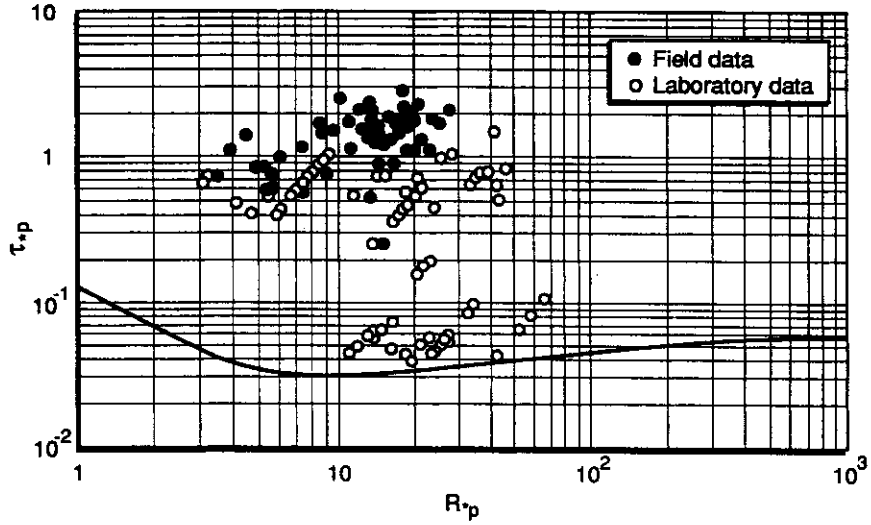

FIG. 6. Shields Diagram for Upper-Regime Plane Bed

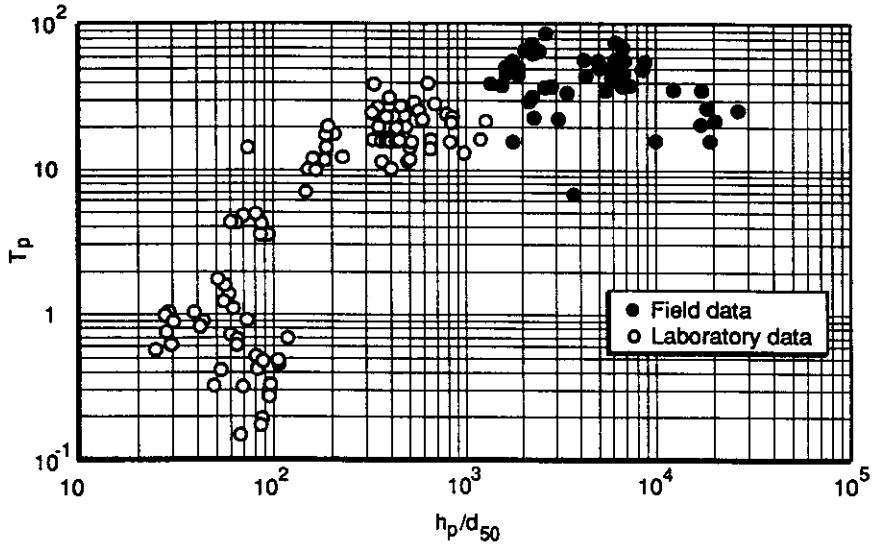

FIG. 7. Transport-Stage Parameter T_p versus Relative Submergence h_p/d_{50} for Upper-Regime Plane Bed

that is not a function of grain diameter is a constant value of $\tau_* d_* = R_*^2/d_*^2$. Moreover, with $G = 2.65$ and the laminar sublayer thickness $\delta = 11.6\nu/u_*$, one demonstrates that the sublayer Froude number $F_* = u_{*p}/\sqrt{g\delta} = 1$ when $\tau_* d_* = 3.674$.

Fig. 9 shows the relationship between τ_{*p} and d_*. The agreement between $\tau_* d_* \cong 4$ and the upper-regime plane bed observations at $R_* < 11.6$ is very good. The physical significance of $\tau_* d_* \cong 4$ for $R_* < 11.6$ can be found in the following: (1) The sublayer Froude number $F_* = u_{*p}/\sqrt{g\delta} = 1$ separates the lower regime $F_* < 1$ and the upper regime $F_* > 1$; and (2) the sublayer Froude number also corresponds to the ratio of the applied bed-shear stress $\tau_p = \rho u_{*p}^2$ to the pressure difference in the laminar sublayer $\Delta p_* = \rho g \delta_p$, hence $\tau_p = \Delta p_*$ when $F_* = 1$. As expected from these conditions, the occurrence of upper-regime plane bed when $R_* < 11.6$ does not depend on grain size.

Equivalent ways to designate upper-regime plane bed when $R_* < 11.6$ in terms of Shields parameter τ_{*p}, shear velocity u_{*p}, or flow depth h_p are, respectively

$$\tau_{*p} d_* \cong 4; \quad u_{*p} \cong 2[(G-1)g\nu]^{1/3}; \quad h_p \cong \frac{4(G-1)d_{50}}{d_* S} \tag{1a-c}$$

These relationships are valid only for the transition to hydraulically smooth boundary, i.e., $4 < R_* < 11.6$, which corresponds to $2 < d_* < 6$, or fine to medium sand.

Transition to Hydraulically Rough Boundary $11.6 < R_* < 70$

In the transition to hydraulically rough boundary $11.6 < R_* < 70$, the presence of sediment of size $d_{50} > \delta$ is expected to perturb the laminar sublayer. There are two possible ways in which the grain size could exert an influence on the laminar sublayer: (1) Through direct influence on the laminar sublayer thickness, e.g., a constant value of d_{50}/δ, or R_{*p}; or (2) through an influence on the relative roughness h_p/d_{50}. Both possibilities are examined subsequently.

In the first case, the lack of observations for upper-regime plane bed when $R_* > 50$ in Fig. 9 suggests that the conditions for upper-regime plane bed are such that $d_{50} \cong 2\delta$, or $R_* \cong 20$. The occurrence of upper-regime plane bed seems physically related to the stability of the laminar sublayer. Given $\tau_{*p} = R_{*p}^2/d^3$, one obtains the following equivalent relationships for the Shields parameter τ_{*p} and the flow depth h_p:

$$R_* \cong 20; \quad \tau_{*p} \cong \frac{400}{d_*^3}; \quad h_p \cong \frac{400(G-1)d_{50}}{S d_*^3} \tag{2a-c}$$

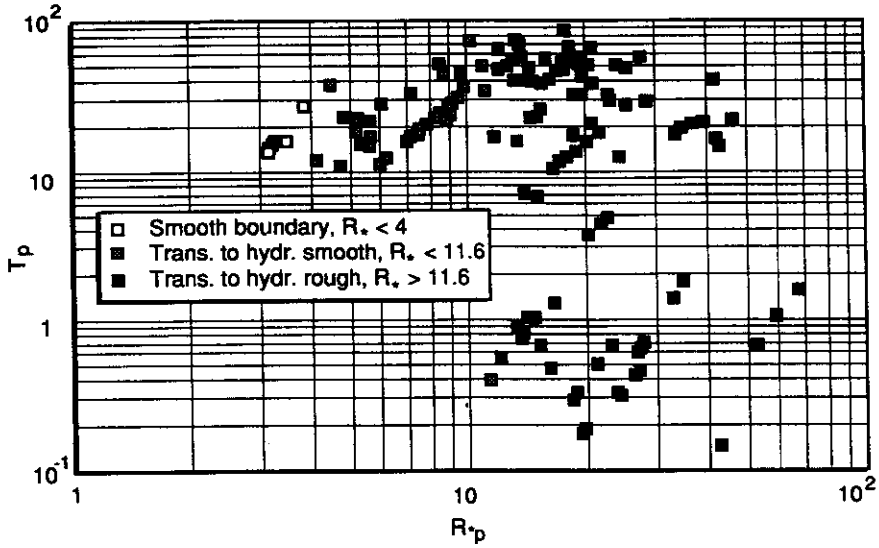

FIG. 8. Transport-Stage Parameter T_p versus Grain Shear Reynolds Number R_{*p} for Upper-Regime Plane Bed

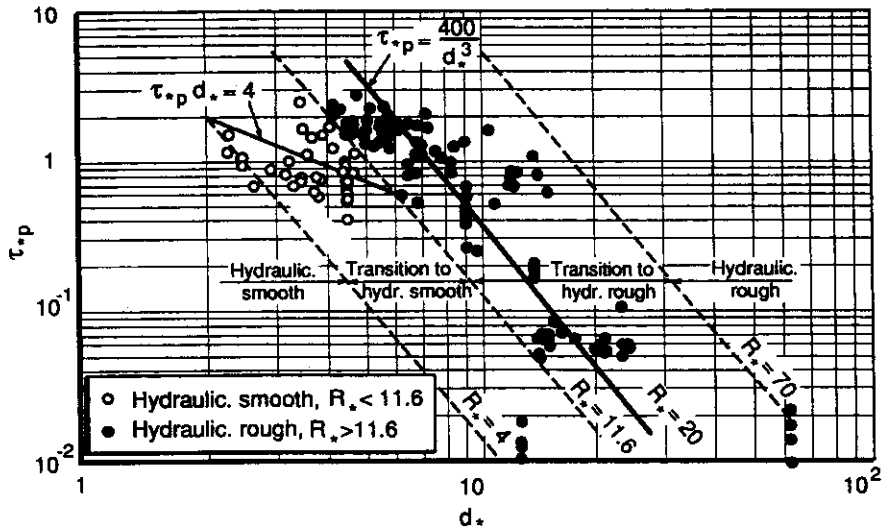

FIG. 9. Shields Parameter τ_{*p} versus Dimensionless Particle Diameter d_* for Upper-Regime Plane Bed

These relationships are valid when $11.6 < R_* < 70$, which corresponds to $4 < d_* < 70$ or medium sand to very fine gravel.

In the second case, the effect of grain size on the flow depth is examined in Fig. 10 by plotting $\tau_{*p}d_*$ versus h_p/d_{50}. It is first observed that when $R_* < 11.6$, the approximation $\tau_{*p}d_* \cong 4$ remains valid regardless of h_p/d_{50}. Also, the value of $\tau_{*p}d_*$ increases with h_p/d_{50} when $R_* > 11.6$. From Fig. 10, the following empirical relationship for transition to hydrauically rough is

$$\tau_{*p}d_* \cong 5.75 \log \frac{h_p}{20d_{50}} \tag{3}$$

Despite significant scatter in Fig. 10, it is shown that $\tau_{*p}d_*$ definitely increases with h_p/d_{50}. For field applications, it is important to notice that a significant increase in $\tau_{*p}d_*$ above the value of 4 is possible at large values of relative submergence when $h_p/d_{50} \gg 500$. Therefore, field measurements where $h_p/d_{50} > 500$ may be significantly different from laboratory conditions when $h_p/d_{50} < 500$.

In terms of resistance to flow over hydraulically rough boundaries, the occurrence of upper-regime plane bed depends on relative roughness, and the results of Fig. 10 corroborate those of Fig. 7.

Temperature Effects

Figs. 9 and 10 are of particular significance because they can explain the intriguing changes in bed-form configurations due to water temperature. For instance, the Missouri River has been known to change bed-form configuration as a function of water temperature given a constant flow discharge (Shen et al. 1978). When $R_* \cong 11.6$, a slight change in water temperature, and thus water kinematic viscosity, changes the bed condition in the transition from hydraulically smooth to hydraulically rough. Temperature effects can therefore be important to change bed-form configurations when the following conditions are satisfied:

1. Grain shear Reynolds number has to be close to the threshold value $R_{*p} \cong 11.6$, such that temperature changes can shift R_{*p} below or above the threshold value.
2. Shields parameter τ_{*p} has to be close to 1, essentially $0.5 < \tau_{*p} < 5$, such that the flow would be in the upper regime if $R_{*p} < 11.6$ and the lower regime if $R_{*p} > 11.6$. This condition is also equivalent to $3 < d_* < 6$, considering $\tau_* d_*^3 = R_*^2$.
3. Relative submergence has to be larger than $h_p/d_{50} > 500$ to see a significant difference between hydraulically

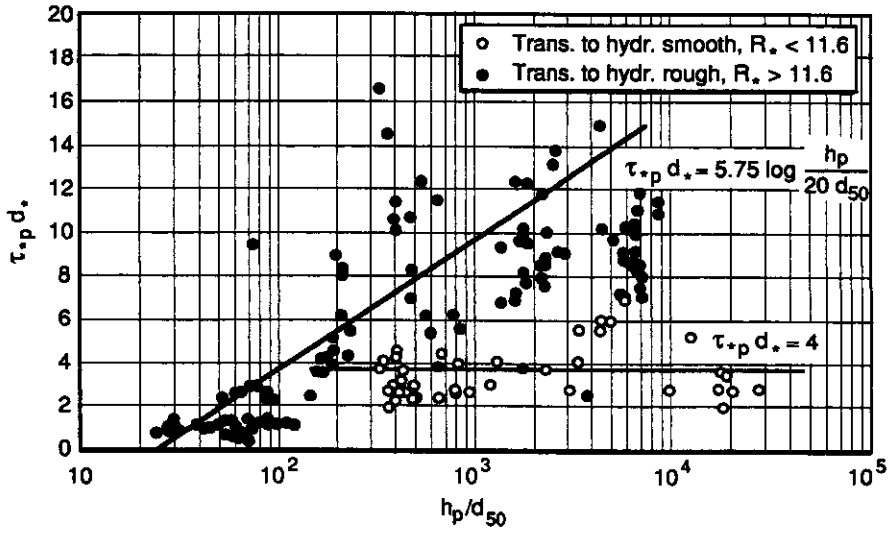

FIG. 10. Diagram of $\tau_{*p}d_*$ versus Relative Submergence h_p/d_{50} for Upper-Regime Plane Bed

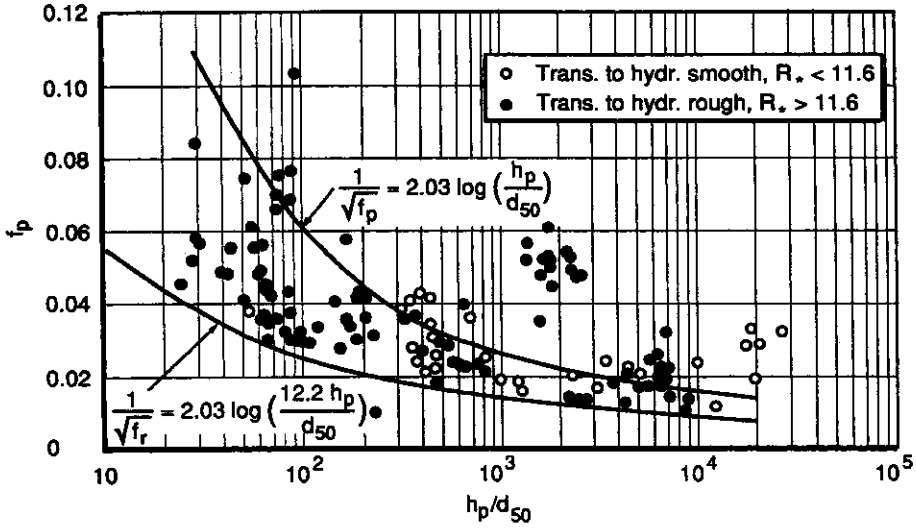

FIG. 11. Darcy-Weisbach Friction Factor f_p versus Relative Submergence h_p/d_{50} for Upper-Regime Plane Bed

smooth and rough plane bed conditions. The differences between boundary conditions become particularly significant for field conditions.

RESISTANCE TO FLOW FOR UPPER-REGIME PLANE BED

Resistance to flow for upper-regime plane bed is analyzed in terms of the Darcy-Weisbach friction factor for the extended data set. The difficulty in the analysis of resistance to flow in sand-bed channels stems from the fact that the boundary condition is neither hydraulically rough nor hydrauically smooth. The laws governing the mechanics of the flow in the transition zone, $4 < R_{*p} < 70$, are still poorly understood. Most existing relationships for grain resistance to flow in sand-bed channels are based on the rigid boundary friction factor f_r for hydraulically rough boundary like the relationship proposed by Keulegan (1938)

$$\sqrt{\frac{1}{f_r}} = 2.03 \log\left(\frac{12.2h_p}{d_{50}}\right) \tag{4}$$

The measured values of the Darcy-Weisbach friction factor for both field and laboratory data are plotted against the relative submergence h_p/d_{50} in Fig. 11. Generally, the figure shows that f decreases with an increase in h_p/d_{50}. Field and laboratory measurements display higher resistance values than calculated with (4) assuming a hydraulically rough rigid boundary. Resistance to flow values for transition to hydraulically smooth boundary are comparable to those for transition to hydraulically rough. Comparisons with the following relationship, and also in Fig. 11, show that an average relationship for the mobile-bed friction factor f_p in the transition region $3 < R_* < 70$:

$$\sqrt{\frac{1}{f_p}} \cong 2.03 \log\left(\frac{h_p}{d_{50}}\right) \tag{5}$$

This relationship is only valid for grain resistance of upper-regime plane bed.

A comparison of the measured mobile bed friction factor f_p to the rigid boundary friction factor f_r calculated from (4) is shown in Fig. 12. When the ratio f_p/f_r is plotted as a function of the Shields parameter, it is found that compared with flow resistance for a fixed rough plane boundary, flow resistance for mobile upper-regime plane bed generally increases as τ_{*p} increases. An empirical relationship gives the ratio between the Darcy-Weisbach friction factor for a mobile plane boundary f_p from the friction factor for a rigid plane boundary f_r and the Shields parameter τ_{*p} as

$$f_p \cong f_r(3 + \log \tau_{*p}) \tag{6}$$

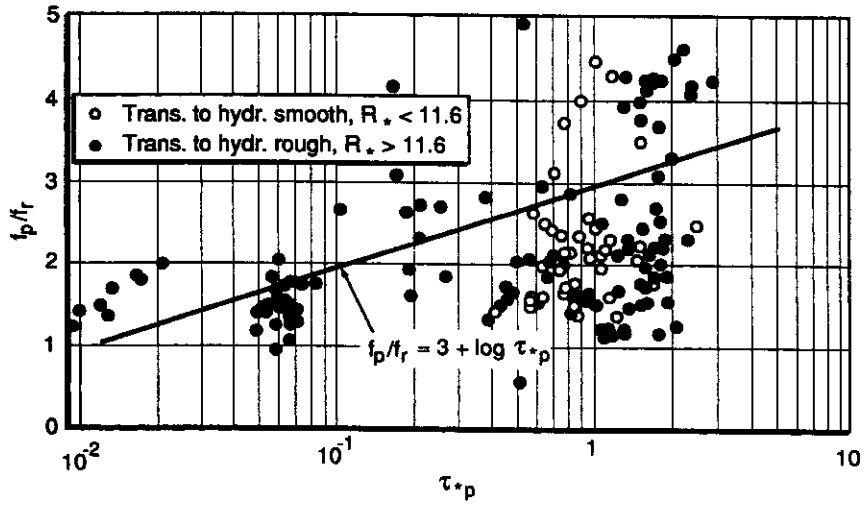

FIG. 12. Ratio of Rigid Bed Resistance f_p/f_r versus Shields Parameter τ_{*p} for Upper-Regime Plane Bed

This relationship is valid for upper-regime plane bed, i.e., when $\tau_{*p} > 0.01$, and only provides an approximation of grain resistance in mobile sand-bed channels because of the substantial scatter observed at higher values of τ_{*p}. Because τ_{*p} describes particle mobility, one can thus infer from Fig. 12 that plane bed resistance to flow increases with sediment transport.

CALCULATION PROCEDURE FOR UPPER-REGIME PLANE BED

The following procedure for the analysis of upper-regime plane bed in sand-bed channels addresses two issues given the flow depth, channel slope, and particle diameter: (1) Under what flow depth can one expect upper-regime plane bed with sediment transport?; and (2) what is the expected value of the Darcy-Weisbach friction factor for upper-regime plane bed?

Part A

Given the energy slope S, the median bed material grain size d_{50}, kinematic viscosity ν, and specific gravity G, determine the flow depth h_p for upper-regime plane bed.

1. Calculate the dimensionless particle diameter $d_* = d_{50}[(G - 1)g/\nu^2]^{1/3}$.
2. Calculate the Shields parameter from $\tau_* = hS/(G - 1)d_{50}$.
3. Calculate the grain shear Reynolds number from $R_* = (\tau_* d_*^3)^{1/2}$.
4. The flow depth for upper-regime plane bed is

$$h_p \cong \frac{4(G - 1)d_{50}}{Sd_*} \quad \text{when } R_* < 11.6$$

or

$$h_p \cong \frac{400(G - 1)d_{50}}{Sd_*^3} \quad \text{when } R_* > 11.6$$

if $3 < d_* < 6$, check for possible water temperature effects (see example below).

Part B

Resistance to fow for upper-regime plane bed can be estimated with two different methods.

1. A first estimate of the friction factor for a mobile plane bed f_p is obtained from

$$f_p = \frac{1}{\left[2.03 \log \frac{h_p}{d_{50}}\right]^2}$$

2. When $\tau_{*p} > 0.01$, resistance to flow for a mobile plane bed f_p can also be estimated from

$$f_p \cong \lfloor 3 + \log \tau_{*p} \rfloor \left[\frac{1}{2.03 \log \frac{12.2h_p}{d_{50}}}\right]^2$$

Neither of these two methods provides very accurate grain resistance factors for upper-regime plane bed with sediment transport in sand-bed channels, owing to the scatter in Figs. 11 and 12.

EXAMPLE—TEMPERATURE EFFECTS OF MISSOURI RIVER

Bed forms in the Missouri River are known to be dependent on water temperature as reported by Chen and Nordin (1976), Shen (1977), and Shen et al. (1978). A calculation example is presented for the Missouri River at a flow depth $h = 10.08$ ft $= 3.07$ m, given the bed material size $d_{50} \cong 0.218$ mm, the energy slope $S \cong 1.42 \times 10^{-4}$, and the kinematic viscosity $\nu = 1.58 \times 10^{-6}$ m^2/s at a water temperature of 3°C.

Part A

The flow regime is identified given h, S, d_{50}, G, and ν. In this case

$$d_* = d_{50}\left[\frac{(G - 1)g}{\nu^2}\right]^{1/3} = 2.18 \times 10^{-4}\left[\frac{1.65 \times 9.81}{(1.58 \times 10^{-6})^2}\right]^{1/3} = 4.06$$

with $3 < d_* < 6$, the Shields parameter, and the grain shear Reynolds number are

$$\tau_* = \frac{hS}{(G - 1)d_{50}} = \frac{3.07 \times 1.42 \times 10^{-4}}{(2.65 - 1)2.18 \times 10^{-4}} = 1.21$$

and

$$R_* = (\tau_* d_*^3)^{1/2} = (1.21 \times 4.06^3)^{1/2} = 9 < 11.6$$

Notice that the reason for this peculiar change in bed-form configuration with changes in water temperature for the Missouri River is due to the near threshold values of d_* and R_*. Indeed, when $3 < d_* < 6$, slight water temperature, and thus

viscosity changes, may switch the values of R_* below or above the threshold value of $R_* = 11.6$.

For $R_* < 11.6$, the upper-regime plane bed flow depth is calculated from

$$h_p = \frac{4(2.65 - 1)2.18 \times 10^{-4}}{4.06 \times 1.42 \times 10^{-4}} = 2.5 \text{ m}$$

At this water temperature, a flow depth $h = 3.07$ m is near the upper-regime plane bed flow depth for transition to hydraulically smooth.

Notice that because $R_* \cong 11.6$, changes in water temperature can change bed-form configurations. Indeed, at the same flow depth, if the water temperature increases to 20°C the calculations can be repeated with a kinematic viscosity of $\nu = 1 \times 10^{-6}$ m²/s. One thus obtains $d_* = 5.5$, $\tau_* = 1.21$, and now $R_* = 14.2 > 11.6$. The corresponding upper-regime flow depth is

$$h_p \cong \frac{400(2.65 - 1)2.18 \times 10^{-4}}{1.42 \times 10^{-4} \times 5.5^3} = 6.1 \text{ m}$$

At a water temperature of 20°C, a flow depth $h = 3.07$ m is in the lower regime and dunes should form. One thus concludes that a change in water temperature in the Missouri River triggers a shift in the flow depth for upper-regime plane bed from 2.5 to 6.1 m. At a flow depth of 3.07 m in the Missouri River, one can thus expect fully developed sand dunes during the summer months, washed-out dunes as water temperature decreases in the fall, and transition to upper regime when the water temperature is cold.

Part B

Resistance to flow for upper-regime plane bed can be approximated for a mobile boundary with $h_p = 2.5$ m as

$$f_p \cong \frac{1}{\left[2.03 \log\left(\frac{2.5}{0.000218}\right)\right]^2} = 0.0147$$

with a value of $\tau_{*p} = 0.98$, the friction factor f_p after considering sediment transport gives

$$f_p \cong [3 + \log 0.98]\left[\frac{1}{2.03 \log \frac{12.2 \times 2.5}{2.18 \times 10^{-4}}}\right]^2 = 0.027$$

These values are within the range of variability in field measurements, as shown in Fig. 11 given $h_p/d_{50} = 11{,}470$.

CONCLUSIONS

Upper-regime plane bed with sediment transport has been examined in the laboratory and with field measurements. The following conclusions can be drawn from the laboratory experiments:

1. The Darcy-Weisbach friction factor f for an equal volume sediment mixture is closer to that of the fine fraction than the coarse fraction. This is corroborated by visual observations that finer fractions fill the interstices between coarse particles on the bed surface and cause effective smoothing of the bed.
2. Upper-regime plane bed is observed in the transition zone between hydraulically rough and hydraulically smooth boundaries, i.e., $4 < R_* < 70$.
3. There is no unique value of the transport-stage parameter T_p that describes upper-regime plane beds. The transport-stage parameter T_p increases with relative submergence h_p/d_{50}.

From the analysis of the field and laboratory data set, the following conclusions can be formulated:

1. Two types of boundary conditions must be analyzed separately as follows:
   a. For the transition to hydraulically smooth boundary ($4 < R_* < 11.6$, or $d_* < 6$), conditions depend on shear velocity and viscosity regardless of grain size. Plane bed is obtained when the laminar sublayer Froude number $F_* = u_*/\sqrt{g\delta} = 1$, which corresponds to $\tau_{*p}d_* \cong 4$.
   b. For the transition to hydraulically rough boundary ($11.6 < R_* < 70$, or $d_* > 3$) conditions depend on grain size, and plane bed is found where $d_{50} \cong 2\delta_p$. This corresponds to $\tau_{*p} \cong 400/d_*^3$. It is also found that $\tau_{*p}d_*$ varies with h_p/d_{50} in Fig. 10.
2. The Darcy-Weisbach friction factor f_p for a mobile plane boundary increases with the Shields parameter τ_{*p}, thus with sediment transport [e.g., (6)].
3. A procedure for the analysis of upper-regime plane bed is presented; the method explains why and when water temperature effects can be important in changing bed-form configuration. Water temperature effects are significant when $R_* \cong 11.6$, and $3 < d_* < 6$. The example of the Missouri River is shown to satisfy these conditions. The proposed procedure explains why bed-form configurations of the Missouri River change with water temperature.

ACKNOWLEDGMENTS

The writers are grateful to Drs. D. K. Sunada and E. V. Richardson at the Water Research Center at Colorado State University for the academic support to the second writer during the course of his PhD study. Discussions with C. F. Nordin, G. J. Klaassen, A. Wijbenga, L. van Rijn, D. B. Simons, P. G. Combs, and C. Fischenich on various aspects of the complex problem of bedforms in sand-bed channels were most stimulating and appreciated.

APPENDIX I. REFERENCES

Athaullah, M. (1968). "Prediction of bedforms in erodible channels," PhD dissertation, Dept. of Civ. Engrg., Colorado State Univ., Fort Collins, Colo.

Beckman, E. W., and Furness, L. W. (1962). "Flow characteristics of Elkhorn River near Waterloo, Nebraska." *Water Supply Paper 1498-B*, U.S. Geological Survey, Washington, D.C.

Bennett, J. P. (1995). "Algorithm for resistance to flow and transport in sand-bed channels." *J. Hydr. Engrg.*, ASCE, 121(8), 578–590.

Best, J. L., and Bridge, J. S. (1992). "The morphology and dynamics of low amplitude bedwaves upon upper-stage plan beds and preservation of planar laminae." *Sedimentology*, 39, 737–752.

Bray, D. I. (1982). "Flow resistance in gravel-bed rivers, in gravel-bed river." *Fluvial processes, engineering and management*, John Wiley & Sons, Inc., New York, 109–137.

Brownlie, W. (1982). Prediction of flow depth and sediment transport in open channels," PhD dissertation, California Inst. of Technol., Pasadena, Calif., 410.

Chen, Y. H., and Nordin, C. F. (1976). "Missouri river temperature effects in the transition from dunes to plane bed." *MRD Sediment Ser. No. 14*, U.S. Army Engr. Dis., Corps of Engrs., Omaha, Neb., 37.

Chyn, S. D. (1935). "An experimental study of the sand transporting capacity of the flowing water on sandy bed and the effect of the composition of the sand," Thesis, MIT, Cambridge, Mass., 33.

Daranandana, N. (1962). "A preliminary study of the effect of gradation of bed material on flow phenomena in alluvial channels," PhD dissertation, Colorado State Univ., Fort Collins, Colo.

Einstein, H. A., and Barbarossa, N. L. (1952). "River channel roughness." ASCE, 117, 1121–1132.

Engelund, F., and Fredsøe, J. (1974). "Transition from dunes to plane bed in alluvial channels," *Ser. Paper 4*, Inst. of Hydrodynamics and Hydr. Engrg., Tech. Univ. of Denmark, Denmark, 56.

Engelund, F., and Hansen, E. (1967). *A monograph on sediment transport in alluvial streams*. TekniskForlag, Copenhagen, Denmark.

Franco, J. J. (1968). "Effects of water temperature on bed load movement." *J. Wtrwy., and Harb. Div.*, ASCE, 94(3), 343–352.

Guy, H. P., Simons, D. B., and Richardson, E. V. (1966). "Summary of alluvial channel data from flume experiments, 1956–61." *Profl. Paper 462-I*, U.S. Geological Survey.
Jorissen, A. L. (1938). "Etude experimentale du transport solide des cours d'eau." *Revue Universelle des Mines*, Belgium, 14(3), 269–282.
Julien, P. Y. (1992). "Study of bedform geometry in large rivers." *Rep. Q 1386*, Delft Hydraulics, 78.
Julien, P. Y. (1995). *Erosion and sedimentation*. Cambridge University Press, 280.
Julien, P. Y., and Klaassen, G. J. (1995). "Sand dune geometry in flooded rivers." *J. Hydr. Engrg.*, ASCE, 121(9), 657–663.
Julien, P. Y., and Klaassen, G. J. (1997). "Closure to discussion of 'Sand dune geometry in flooded rivers,' by Mario L. Amsler and Marcelo H. García." *J. Hydr. Engrg.*, ASCE, 123(6), 582–585.
Julien, P. Y., Lan, Y. Q., and Berthault, G. (1993). "Experiments on stratification of heterogeneous sand mixtures." *Bull. de la Société Géologique de France*, France, 164(5), 649–660.
Kamphuis, J. W. (1974). "Determination of sand roughness for fixed beds." *J. Hydr. Res.*, 12(2), 193–203.
Keulegan, G. H. (1938). "Laws of turbulent flows in open channels." *J. Nat. Bureau of Standards*, 21, 707–741.
Klaassen, G. J. (1991). "Experiment on the effect of gradation and vertical sorting on sediment transport phenomena in the dune phase." *Proc., Grain Sorting Seminar*, 127–145.
Meyer-Peter, E., and Müller, R. (1948). "Formulas for bed load transport." *Proc., 2nd Meeting Int. Assn. for Hydr. Struct. Res.*, 26.
Nnadi, F. N., and Wilson, K. C. (1995). "Bed-load motion at high shear stress: Dune washout and plane-bed flow." *J. Hydr. Engrg.*, ASCE, 121(3), 267–273.
Nordin, C. F., Jr. (1964). "Aspects of flow resistance and sediment transport, Rio Grande near Bernalillo, New Mexico." *Water Supply Paper 1498-H*, U.S. Geological Survey, Washington, D.C.
Nordin, C. F., Jr. (1965). "Sediment transport in the Rio Grande, New Mexico." *Profl. Paper 462-F*, U.S. Geological Survey, Washington, D.C., 35.
Nordin, C. F., Jr. (1976). "Flume studies with fine and coarse sands." *Open File Rep. 76-762*, U.S. Geological Survey, Washington, D.C., 18.
Paola, C., Wiele, S. M., and Reinhart, M. A. (1989). "Upper-regime parallel lamination as a result of turbulent sediment transport and low-amplitude bedforms." *Sedimentology*, 36, 47–59.
Raslan, Y. (1994). "Resistance to flow in the upper-regime plane bed," PhD dissertation, Dept. of Civ. Engrg., Colorado State Univ., Fort Collins, Colo., 135.
"Sedimentation engineering." (1997). *Manual and Rep. on Engrg. Prac. No. 65*, ASCE, New York, 745.
Shen, H. W. (1977). "Analyses of temperature effects on stage-discharge relationship in a Missouri river reach near Omaha." *MRD Sediment Ser. No. 15*, U.S. Army Engr. Div., Missouri River, Corps of Engrs., Omaha, Neb., 43.
Shen, H. W., Mellema, W. J., and Harrison, A. S. (1978). "Temperature and Missouri river stages near Omaha." *J. Hydr. Div.*, ASCE, 104(1), 1–20.
Simons, D. B., and Richardson, E. V. (1961). "Forms of bed roughness in alluvial channels." *J. Hydr. Div.*, ASCE, 87(3), 87–105.
Simons, D. B., and Richardson, E. V. (1966). "Resistance to flow in alluvial channels." *Profl. Paper No. 422-J*, U.S. Geological Survey.
Simons, D. B., and Senturk, F. (1992). *Sediment transport technology*. Water Resour. Publ., Fort Collins, Colo.
Singh, B. (1960). "Transport of bed load in channels with special reference to gradient form," PhD dissertation, Univ. of London, London.
U.S. Army Corps of Engineers (USACE). (1936a). "Flume tests made to develop a synthetic sand which will not form ripples when used in movable-bed models." *Tech. Memo. 99-1*, U.S. Wtrwy. Experiment Station, Vicksburg, Miss., 21.
U.S. Army Corps of Engineers (USACE). (1936b). "Flume tests of synthetic sand mixture (Sand No. 10)." *Tech. Memo. 95-1*, U.S. Wtrwy. Experiment Station, Vicksburg, Miss., 21.
U.S. Army Corps of Engineers (USACE). (1969). "Missouri river channel regime studies." *MRD Sediment Ser. No. 13B*, Omaha Dis., Omaha, Neb.
Vanoni, V. A., and Brooks, N. H. (1957). "Laboratory studies of the roughness and suspended load of alluvial streams." *MRD Sediment Ser. No. 11*, Sedimentation Lab., California Inst. of Technol., Pasadena, Calif., 121.
van Rijn, L. D. (1982). "Equivalent roughness of alluvial bed." *J. Hydr. Div.*, ASCE, 108(10), 1215–1218.
van Rijn, L. D. (1984). "Sediment transport. III: Bedforms and alluvial roughness." *J. Hydr. Engrg.*, ASCE, 110(12), 1733–1754.
Wang, Z., and Larsen, P. (1994). "Turbulent structure of water and clay suspensions with bed load." *J. Hydr. Engrg.*, ASCE, 120(5), 577–600.
Wijbenga, J. H. A. (1990). "Flow resistance and bedform dimensions for varying flow conditions—A literature review (main text) and (annexes)." *Rep. on Literature Study, A58*, Delft Hydraulics.
Wijbenga, J. H. A., and Klaassen, G. J. (1983). "Changes in bedform dimensions under unsteady flow conditions in a straight flume." Spec. Publ., Int. Assn. of Sedimentologists, 6, 35–48.
Williams, G. P. (1970). "Flume width and water depth effects in sediment transport experiments." *Profl. Paper No. 562-H*, U.S. Geological Survey.
Znamenskaya, N. S. (1969). "Morphological principle of modeling of river-bed processes." *Proc., 13th Congr. of IAHR*, Vol. 5, 1.

APPENDIX II. NOTATION

The following symbols are used in this paper:

d_{50} = median grain size;
d_* = dimensionless particle diameter;
F = Froude number;
F_* = sublayer Froude number, $\mathsf{F}_* = u_*/\sqrt{g\delta}$;
f_b = bed friction factor;
G = specific gravity;
g = gravitational acceleration;
h = flow depth;
k_s = surface roughness;
Q = flow discharge;
R_* = grain shear Reynolds number, $\mathsf{R}_* = u_* d_{50}/\nu$;
R_b = bed hydraulic radius;
S = friction slope;
T = transport-stage parameter, $T = (\tau_0' - \tau_c)/\tau_c$;
$T°$ = water temperature;
U = mean flow velocity;
u_* = shear velocity;
δ = laminar sublayer thickness, $\delta = 11.6\nu/u_*$;
ν = kinematic viscosity of water;
ρ = mass density of water;
τ_c = critical shear stress for beginning of motion;
τ_0 = bed-shear stress; and
τ_* = Shields parameter, $\tau_* = R_b S/(G - 1)d_{50} = u_*^2/(G - 1)gd_{50}$.

Subscripts and Superscripts

f_p = bed friction factor for upper-regime plane bed;
f_r = bed friction factor for rigid boundary;
f' = grain resistance;
f'' = bed-form resistance; and
p = upper-regime plane bed.